Supporting information

Roles of structural defects in polycrystalline platinum nanowires for enhanced Oxygen Reduction Activity

Xiao Zhao,[1,2]* Shinobu Takao,[2] Yusuke Yoshida,[2] Takuma Kaneko,[2] Takao Gunji,[2] Kotaro Higashi,[2] Tomoya Uruga,[2,3] and Yasuhiro Iwasawa[2,4]*

[1]Key Laboratory of Automobile Materials of MOE, School of Materials Science and Engineering, Jilin University, Changchun 130012, China

[2]Innovation Research Center for Fuel Cells, The University of Electro-Communications, Chofugaoka, Chofu, Tokyo 182-8585, Japan

[3]Japan Synchrotron Radiation Research Institute, SPring-8, Sayo, Hyogo 679-5198, Japan

[4]Graduate School of Informatics and Engineering, The University of Electro-Communications, Chofugaoka, Chofu, Tokyo 182-8585, Japan

*Corresponding author.

E-mail address: xzhao417@jlu.edu.cn; iwasawa@pc.uec.ac.jp

Electrochemical Measurements at Rotating Disk Electrode (RDE): A 0.1 M $HClO_4$ solution was prepared by perchloric acid and 18.2 MΩ·cm Millipore water. Electrocatalyst ink consists of 1 mg electrocatalyst, 0.5 mL Millipore water, 0.4 mL isopropanol, 0.005 ml 5 wt% Nafion®. Pt foil and an RHE were used as counter and reference electrodes, respectively. Electrocatalyst-coated RDEs were prepared by a spin-coating method on a 5 mm RDE. The sequence of electrochemical measurements was as follows: (1) CV conditioning between 0.02 and 1.2 V_{RHE} at 100 mV s^{-1} in N_2-saturated 0.1 M $HClO_4$; (2) base CV at 50 mV s^{-1} in N_2-saturated 0.1 M $HClO_4$; (3) anodic polarization from 0.0 to 1.05 V at 20 mV s^{-1} in O_2-saturated 0.1 M $HClO_4$ at 1600 rpm; (4) measurement of solution resistance by an i-interrupter method for IR compensation; (5) CO stripping test that includes two parts: first, the preadsorption of CO by a chronoamperometry procedure at 0.4 V_{RHE} in CO-saturated 0.1 M $HClO_4$ solution for 5 min and subsequently removal of residual CO by bubbling N_2 for 15 min; second, the preadsorbed CO on Pt was electrooxidized by two potential cycles from 0.025 to 1.2 V_{RHE} at 50 mV s^{-1}, where the second cycle was conducted to check whether the preadsorbed CO was removed completely. The CO stripping Coulombic charges were used for the calculation of electrochemical surface areas.

The structural examination after ORR electrocatalysis: To examine possible structural changes of PPNWs during the whole electrochemical test, the TEM and

HRTEM measurement were conducted after ORR electrocatalysis. The measurement procedure for PPNWs-based RDE electrodes is as follows: (1) CV conditioning between 0.02 and 1.2 V_{RHE} at 100 mV s^{-1} in N_2-saturated 0.1 M $HClO_4$ to obtain stable voltammograms curves (usually 50 cycles); (2) three cycles of CV at 50 mV s^{-1} in N_2-saturated 0.1 M $HClO_4$ electrolyte; (3) ORR electrocatalysis by an anodic polarization from 0.0 to 1.05 V at 20 mV s^{-1} in O_2-saturated 0.1 M $HClO_4$ electrolyte at 1600 rpm (repeating three times). (4) After ORR electrocatalysis, electrocatalysts on RDE were then transferred to grids made of lacey carbon films on copper for TEM and HRTEM analysis.

In-situ X-ray Absorption Fine Structure (XAFS)[44]: The RDE working electrode was used for *in situ* XAFS measurements, similar to our previous reports.[1-3] The *in-situ* XAFS measurement procedure for PPNWs-based RDE electrodes is as follows: (1) CV conditioning between 0.02 and 1.2 V_{RHE} at 100 mV s^{-1} in N_2-saturated 0.1 M $HClO_4$ to obtain stable voltammograms curves (usually 50 cycles); (2) three cycles of CV at 50 mV s^{-1} in N_2-saturated 0.1 M $HClO_4$ electrolyte; (3) the anodic polarization from 0.0 to 1.05 V at 20 mV s^{-1} in O_2-saturated 0.1 M $HClO_4$ electrolyte at 1600 rpm (repeating three times). (4) Measurement of *in-situ* XAFS at set potentials (e.g., 0.4, 0.7, and 0.9 V_{RHE}), at each set potential, the electrodes were first polarized for 5 min to make electrodes enter to a quasi-steady state. Then *in-situ* X-ray absorption signals were collected. Potential-dependent *in situ* XAFS spectra at the Pt L_3-edge were acquired in a fluorescence mode. We used a Si(111) double-crystal monochromator, an ion chamber (I_0: Ar 5% / N_2 95%) for incident X-rays, and a 21 Ge-element detector for fluorescent X-rays at the BL36XU station in SPring-8.[44] XANES spectra were treated by Athena software[4]. Theoretical phase shifts and amplitude functions for EXAFS fitting analysis were calculated from FEFF 8.4.[5] The extracted EXAFS oscillations were k^2-weighted and Fourier-transformed to R space, and the fitting of k^2-weighted EXAFS data in R space were carried out with Artemis.[44]

Aberration-Corrected Electron Microscopy (AC-EM): The electrocatalysts were ultrasonically dispersed in ethanol solution and dropped onto the grids made of lacey

carbon films on copper for AC-EM specimen. AC-EM images were obtained using JEM-ARM002F at 200 kV. Partially, TEM images were obtained using a JEM-2100F.

X-ray Photoelectron Spectra (XPS): Pt 4f XPS spectra were measured with a JEOL JPS-9200 using Mg Kα radiation at 10 kV and 10 mA as an excitation source. The binding energies were referred to 284.5 eV of C 1s level in a graphitic state. Electrocatalyst coated on a glassy carbon plate was used as the electrochemical working electrode and XPS specimen. After the electrochemical activation (usually 50 cycles of CVs), the electrode was washed and subsequently covered by N_2-saturated deionized water for XPS measurement.

X-ray fluorescence (XRF): XRF analysis for the bulk composition was conducted using Rigaku ZSX Primus2.

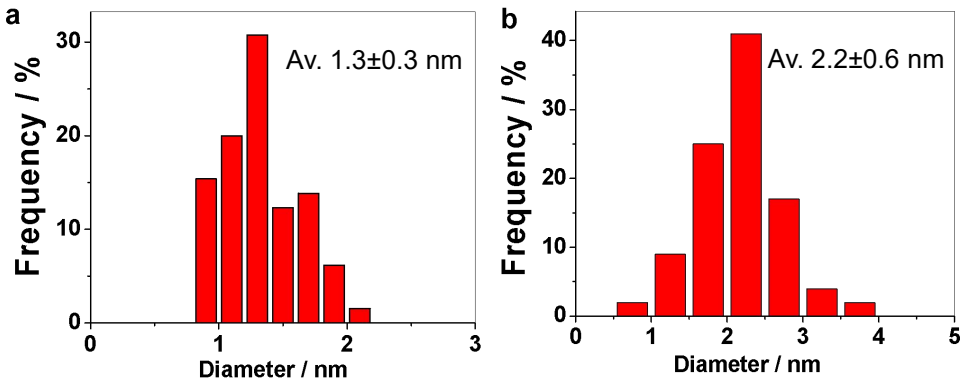

Figure S1. Distribution of nanowires diameter for (a) regular PPNWs and (b) waved PPNWs.

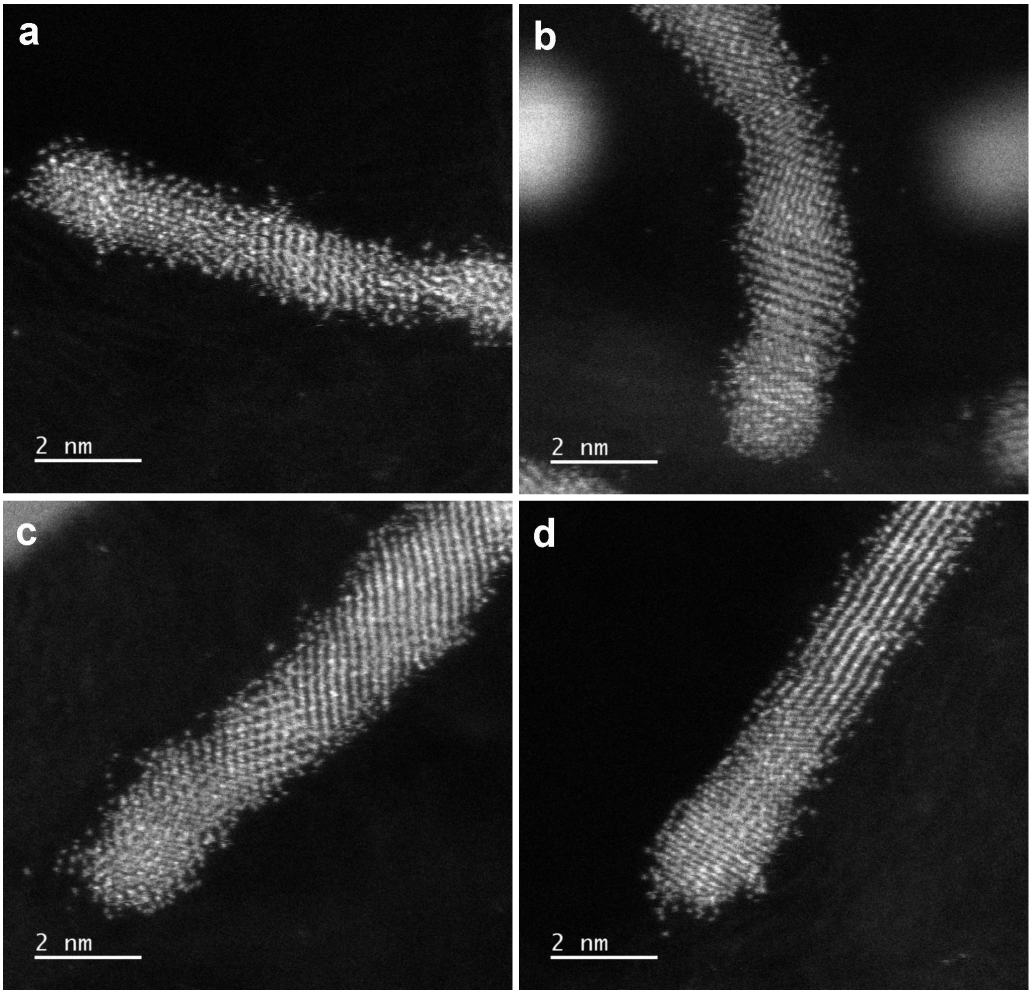

Figure S2. Supplementary atomistic HAADF-STEM images of regular PPNWs that show roughed surfaces instead of flat surfaces. Regardless of these specific nanostructures of PPNWs, two kinds of defects, i.e. in-plane steps and grain boundaries, are generally presented in all randomly-selected PPNWs.

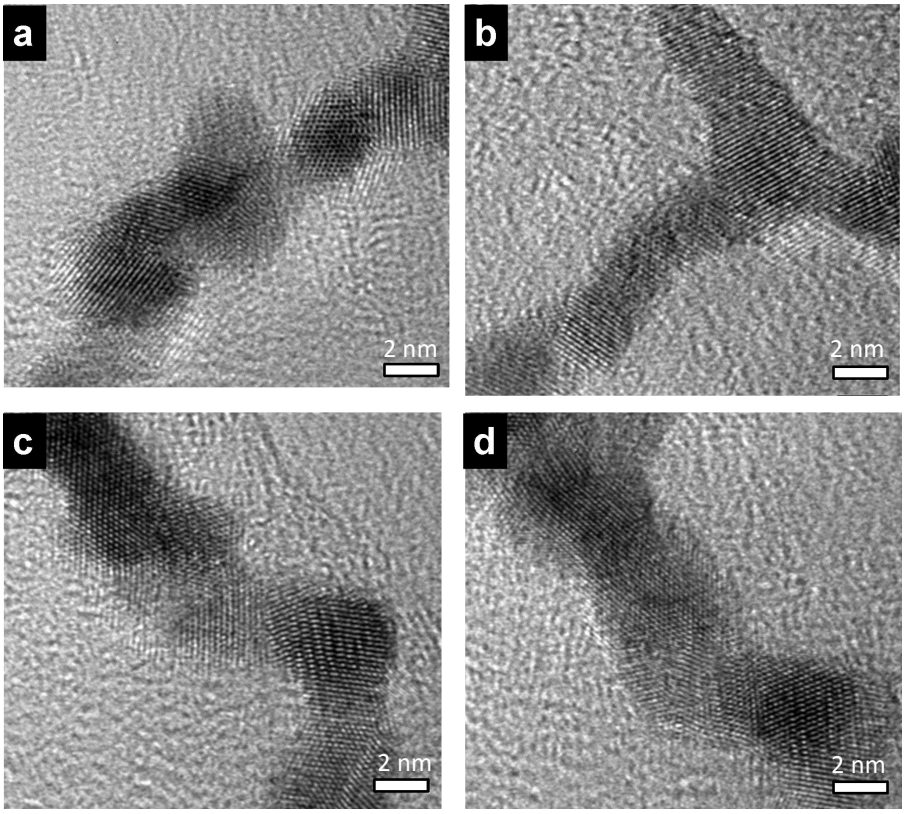

Figure S3. Supplementary atomistic TEM images of waved PPNWs that show the larger orientation freedom for gains and larger misorientation angles of GBs compared to regular PPNWs.

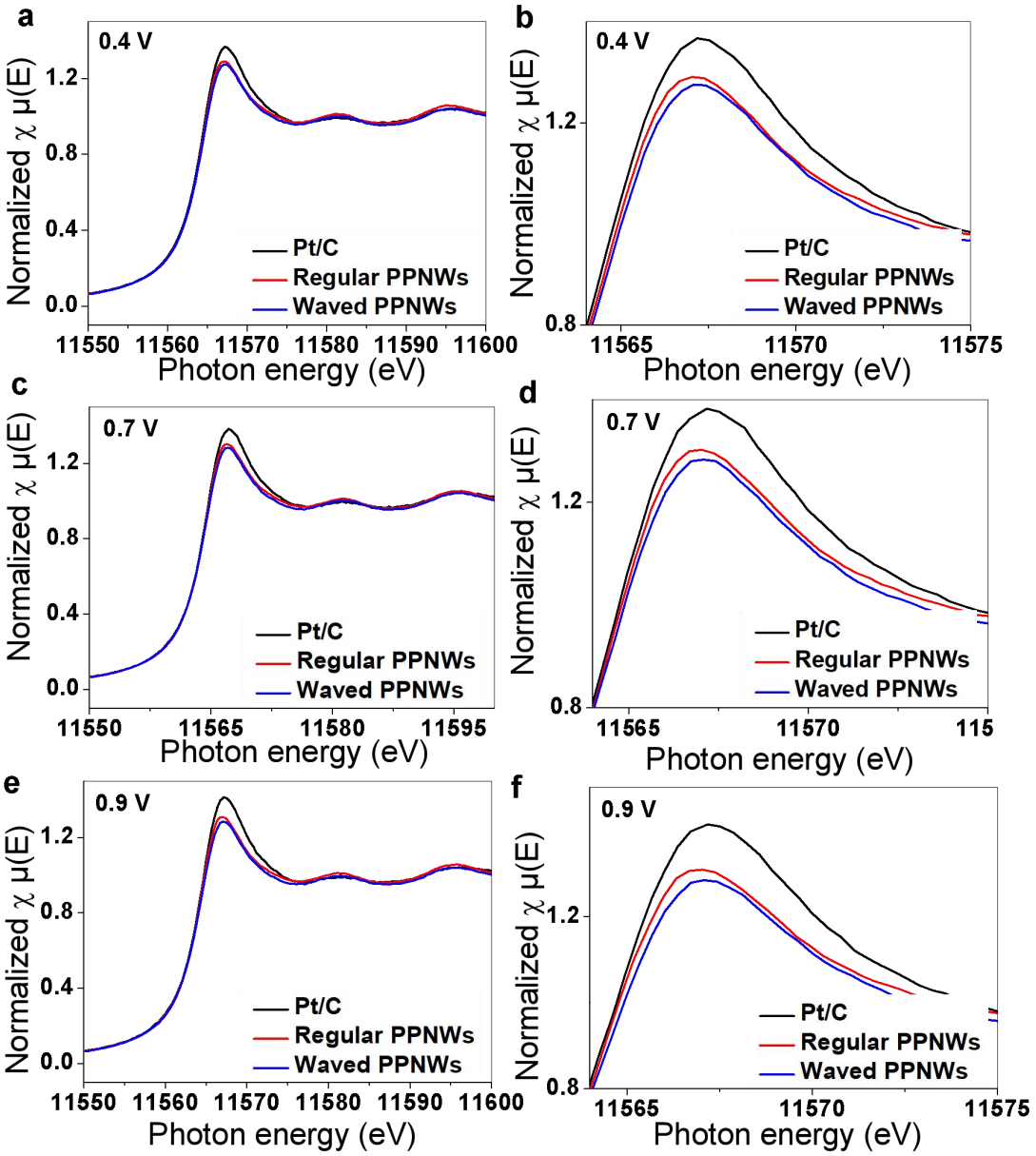

Figure S4. (a-f) *In situ* XANES spectra at Pt L_3-edge for 2 nm Pt/C and regular and waved PPNWs at applied potentials of 0.4, 0.7 and 0.9 V_{RHE}; the zoom-in figures in (b, d, f) highlight the difference in the white-line intensity between three electrodes.

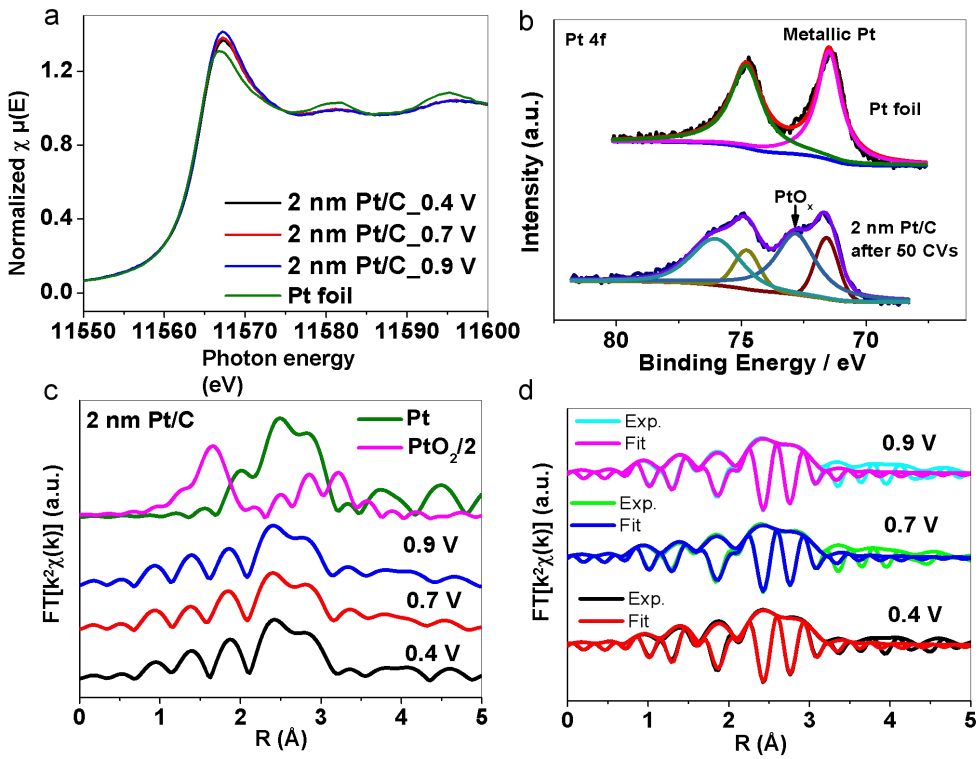

Figure S5. (a) *In situ* potential-dependent XANES at Pt-L_3 edge for 2 nm Pt/C. (b) XPS spectra for Pt foil and 2 nm Pt/C after 50 cycles of cyclic voltammetry, which shows the presence of surface oxide on 2 nm Pt NPs. (c) *In situ* EXAFS Fourier transforms at Pt-L_3 edge for the 2 nm Pt/C at 0.4, 0.7 and 0.9 V_{RHE}. (d) The best fits of FT-EXAFS for 2 nm Pt/C require both Pt-Pt and Pt-O scattering shells (see Table S1 also).

Note: The 2 nm Pt/C has a high occupancy of undercoordinated edge and kinks sites among surface atoms. However, those sites bind oxygen strongly and make almost no positive contribution to the whole ORR activity. By contrast, atomic steps on stepped nanofacets destabilize *OH species via disturbing co-adsorbed interfacial H_2O* networks.[1, 6]

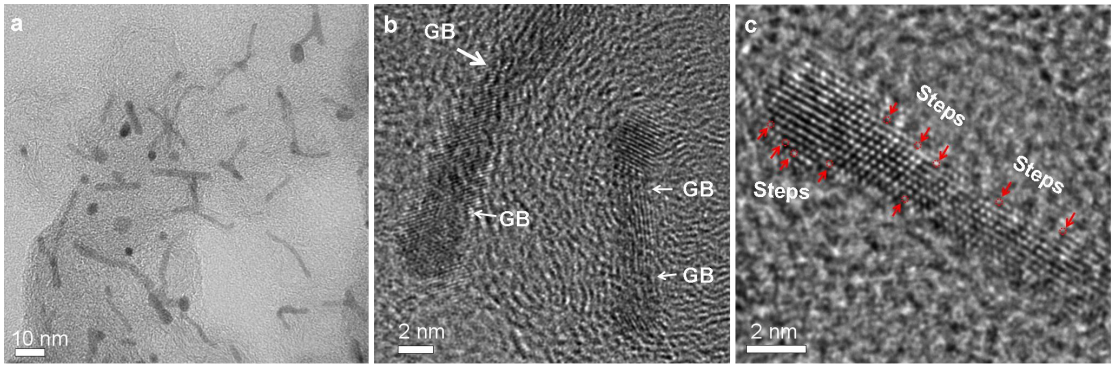

Figure S6. The TEM (a) and HR-TEM (b, c) images for regular polycrystalline Pt nanowires after the ORR electrocatalysis.

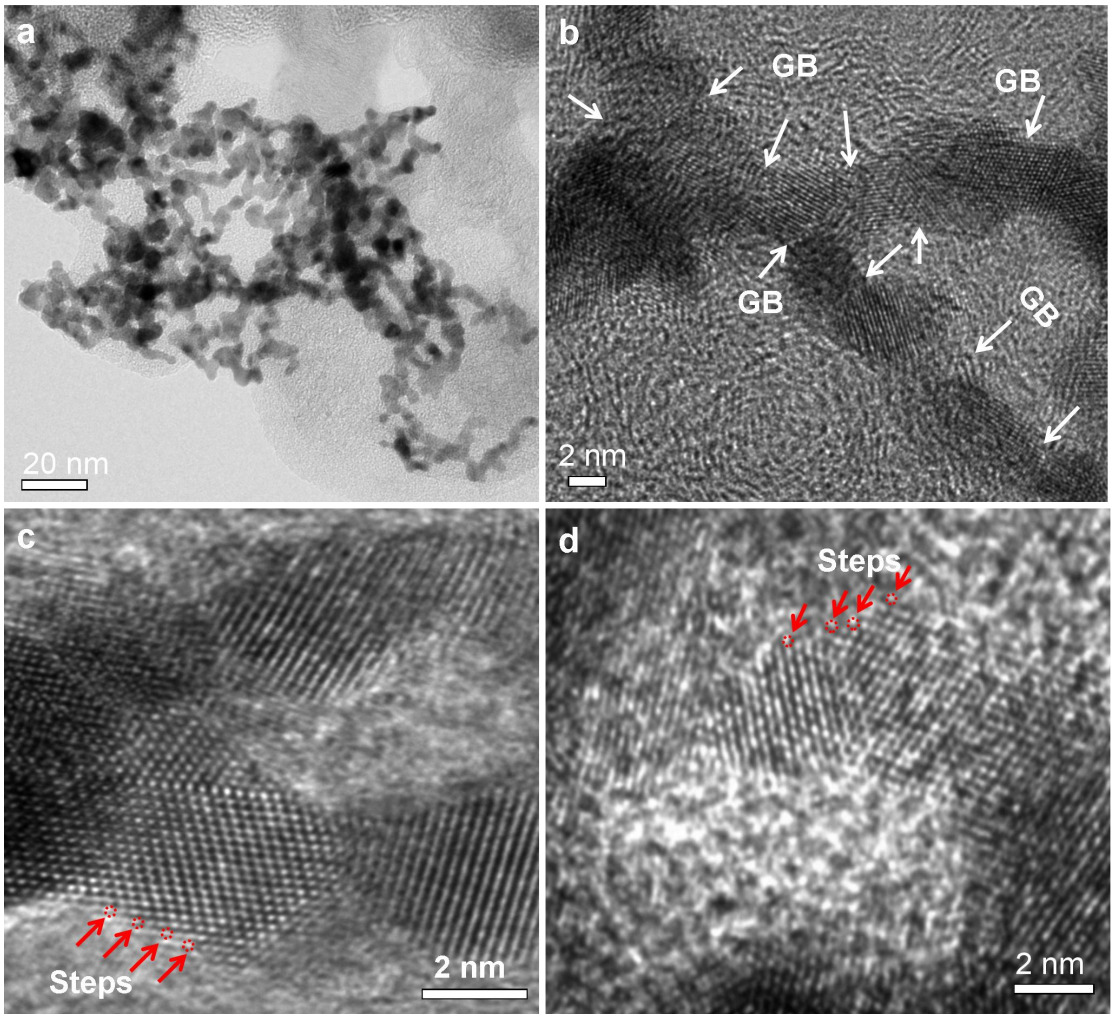

Figure S7. The TEM (a) and HR-TEM (b-d) images for waved polycrystalline Pt nanowires **after the ORR electrocatalysis**.

Table S1. *In situ* EXAFS analysis of 2 nm Pt/C electrode from 0.4 V_{RHE} to 0.7 V_{RHE} and to 0.9 V_{RHE} ; Δ k： 3 - 12 Å, Δ R: 1.4 - 3.0 Å.

Electrode-Potential	Pt-Pt scattering			Pt-O scattering			ΔE_0 / eV	R-factor
	CN	R / Å	$\sigma^2/10^{-3}$ Å^2	CN	R / Å	$\sigma^2/10^{-3}$ Å^2		
2 nm Pt/C-0.4 V	10.9 ± 2.3	2.751±0.024	4 ± 2				4.6±4.6	0.03
2 nm Pt/C-0.4 V	8.3 ± 2.1	2.755±0.030	2 ± 2	1.5±2.5	2.013±0.059	9 ± 23	5.5±6.5	0.006#
2 nm Pt/C-0.7 V	11.0 ± 2.6	2.743±0.026	5 ± 3				3.4±4.7	0.04
2 nm Pt/C-0.7 V	8.8 ± 1.6	2.749±0.021	3 ± 2	1.0±0.4	2.032±0.034	3^	4.6±4.3	0.009#
2 nm Pt/C-0.9 V	11.2 ± 2.1	2.75±0.01	10± 6				-1.5±3.8	0.08
2 nm Pt/C-0.9 V	8.4 ± 1.1	2.741±0.016	2 ± 1.4	1.0±0.3	2.0±0.025	3^	3.1±3.3	0.004#

Fitting goodness is significantly improved with the inclusion of a Pt-O scattering path over without it.
^ Fit was firstly done with a free σ^2

R: interatomic distance; CN: coordination number; σ^2: Debye-Waller factor; ΔE_0: correction of edge energy; R-factor: residual factor

Note: The R-factors (the fitting reliability) for the fits with only a Pt-Pt scattering path are all larger than 2%, but the R-factors were remarkably improved by almost a magnitude order with inclusion of a Pt-O scattering shell, thereby indicating the rationality for the presence of discrete surface oxides on 2 nm Pt/C even at the low potential of 0.4 V. These results are not surprised but in line with our XANES and XPS observations as well as the literature that the steps bind *OH more strongly than Pt(111),[6] and *OH would adsorb on the steps at very low potentials around 0.2 V.[7] Our analysis suggests that the undercoordinated edge and kink sites in the 2 nm Pt/C are inactive or low active for ORR.

Table S2. *In situ* EXAFS analysis of regular PPNWs electrode from 0.4 V_{RHE} to 0.7 V_{RHE} and to 0.9 V_{RHE} ; Δ k : 2.5 – 14.3 Å, Δ R: 1.3 - 3.5 Å.

Electrode-Potential	Pt-Pt scattering			Pt-O scattering			ΔE_0 / eV	R-factor
	CN	R / Å	$\sigma^2/10^{-3}$ Å^2	CN	R / Å	$\sigma^2/10^{-3}$ Å^2		
Regular NWs-0.4 V	10.7 ± 2.4	2.755±0.009	4 ± 0.9				2.5±2.9	0.008
Regular NWs-0.7 V	10.0 ± 2.2	2.754±0.011	3 ± 0.9				2.1±3.5	0.008
Regular NWs-0.9 V	10.4 ± 2.3	2.761±0.013	4 ± 0.7				4.0 ± 4.0	0.007

R: interatomic distance; CN: coordination number; σ^2: Debye-Waller factor; ΔE_0: correction of edge energy; R-factor: residual factor

Table S3. *In situ* EXAFS analysis of waved PPNWs electrode from 0.4 V_{RHE} to 0.7 V_{RHE} and to 0.9 V_{RHE} ; Δ k : 3.0 – 12.0 Å, Δ R: 1.4 - 3.0 Å.

Electrode-Potential	Pt-Pt scattering			Pt-O scattering			ΔE_0 / eV	R-factor
	CN	R / Å	$\sigma^2/10^{-3}$ Å^2	CN	R / Å	$\sigma^2/10^{-3}$ Å^2		
Waved NWs-0.4 V	11.0 ± 1.0	2.758±0.007	4 ± 0.6				5.5±1.4	0.0017
Waved NWs-0.7 V	10.3 ± 0.4	2.755±0.003	5 ± 0.3				4.7±0.5	0.0003
Waved NWs-0.9 V	10.0 ± 0.6	2.754±0.004	5 ± 0.4				4.4 ± 0.8	0.0007

R: interatomic distance; CN: coordination number; σ^2: Debye-Waller factor; ΔE_0: correction of edge energy; R-factor: residual factor.

References:

[1] X. Zhao, T. Gunji, T. Kaneko, Y. Yoshida, S. Takao, K. Higashi, T. Uruga, W. He, J. Liu, Z. Zou, An Integrated Single-Electrode Method Reveals the Template Roles of Atomic Steps: Disturb Interfacial Water Networks and Thus Affect the Reactivity of Electrocatalysts, J. Am. Chem. Soc., 141 (2019) 8516-8526.

[2] X. Zhao, S. Takao, K. Higashi, T. Kaneko, G. Samjeskè, O. Sekizawa, T. Sakata, Y. Yoshida, T. Uruga, Y. Iwasawa, Simultaneous Improvements in Performance and Durability of an Octahedral PtNix/C Electrocatalyst for Next-Generation Fuel Cells by Continuous, Compressive, and Concave Pt Skin Layers, ACS Catal., 7 (2017) 4642-4654.

[3] K. Nagasawa, S. Takao, S.-i. Nagamatsu, G. Samjeské, O. Sekizawa, T. Kaneko, K. Higashi, T. Yamamoto, T. Uruga, Y. Iwasawa, Surface-Regulated Nano-SnO2/Pt3Co/C Cathode Catalysts for Polymer Electrolyte Fuel Cells Fabricated by a Selective Electrochemical Sn Deposition Method, J. Am. Chem. Soc., 137 (2015) 12856-12864.

[4] B. Ravel, M. Newville, ATHENA, ARTEMIS, HEPHAESTUS: data analysis for X-ray absorption spectroscopy using IFEFFIT, J. Synchrotron Radiat., 12 (2005) 537-541.

[5] S.I. Zabinsky, J.J. Rehr, A. Ankudinov, R.C. Albers, M.J. Eller, Multiple-scattering calculations of x-ray-absorption spectra, Phys. Rev. B, 52 (1995) 2995-3009.

[6] I.E.L. Stephens, A.S. Bondarenko, U. Gronbjerg, J. Rossmeisl, I. Chorkendorff, Understanding the electrocatalysis of oxygen reduction on platinum and its alloys, Energy Environ. Sci. , 5 (2012) 6744-6762.

[7] V. Climent, N. Garcia-Araez, E. Herrero, J. Feliu, Potential of zero total charge of platinum single crystals: A local approach to stepped surfaces vicinal to Pt(111), Russ. J. Electrochem. , 42 (2006) 1145-1160.